UDC 532.542
DOI: 10.15587/1729-4061.2017.103880

INVESTIGATION OF FLOW STRUCTURE AND HEAT EXCHANGE FORMATION IN CORRUGATED PIPES AT TRANSIENT REYNOLDS NUMBERS

O. Baskova
Postgraduate student
Department of Nuclear Power Plants and Engineering Thermophysics
National Technical University of Ukraine "Igor Sikorsky Kyiv Polytechnic Institute"
Peremohy ave., 37, Kyiv, Ukraine, 03056
E-mail: BaskAleksandra@gmail.com

G. Voropaiev
Doctor of Physical and Mathematical Sciences, Professor, Head of Department
Department of Hydrobionics and Boundary Layer Control
Institute of Hydromechanics
National Academy of Sciences of Ukraine
Zhelyabova str., 8/4, Kyiv, Ukraine, 03057
E-mail: voropaiev.gena@gmail.com

Досліджено залежність локальної тепловіддачі і довжини початкової ділянки від режиму течії, теплофізичних характеристик теплоносія, геометрії поверхні труби і напрямку теплового потоку. Визначено числа Рейнольдса, за яких виникає нестійкість потоку в трубі при неізотермічній постановці задачі. Розглянуто вплив довжини хвилі гофрованої поверхні труби на зміну структури течії в западині і на процеси тепломасообміну

Ключові слова: гофрування, перехідний режим, течія в трубі, інтенсифікація тепловіддачі, гідравлічний опір

Исследована зависимость локальной теплоотдачи и длины начального участка от режима течения, теплофизических характеристик теплоносителя, геометрии поверхности трубы и направления теплового потока. Определены числа Рейнольдса, при которых возникает неустойчивость потока в трубе при неизотермической постановке задачи. Рассмотрено влияние длины волны гофрированной поверхности трубы на изменение структуры течения во впадине и на процессы тепломассообмена

Ключевые слова: гофрирование, переходной режим, течение в трубе, интенсификация теплоотдачи, гидравлическое сопротивление

1. Introduction

Intensification of heat exchange processes in the elements of power equipment at equal heat exchange areas and equal velocities of the same coolant (that is, when the Reynolds and Prandtl numbers are equal) is determined by the structure of the coolant flow on the heat exchange surfaces. The flow structure is understood as thickness of the dynamic boundary layer or flow conditions in the boundary layer (laminar or turbulent flow) or spatial and time scales of the vortex perturbations in the boundary layer and intensity of these perturbations.

Heat exchange can be intensified by realization of Reynolds analogy through increase of stresses on the streamlined surface and thereby intensity of the vortex structures in the boundary layer. However, this process is energy-consuming [1]. There are many examples of such surfaces (for example, a rough surface) but unfortunately their effectiveness is usually small.

Structured surfaces of heat exchangers realizing generation of near-wall vortex structures of a specified type and scale enable minimization of energy costs per unit of change in intensity of heat exchange.

Structuring of streamlined surfaces is one of the most common methods of heat exchange intensification to date. Corrugation is a special case of this method; it ensures a significant increase of efficiency of the heat exchange equipment by intensifying vortex perturbations on streamlined surfaces. Intensity of heat removal and growth of hydraulic resistance accompanying corrugation depend in a quite complicated way on geometric parameters of the corrugated surface when the Reynolds and Prandtl numbers vary.

2. Literature review and problem statement

There are many published works devoted to analysis of influence of the corrugated surface geometry parameters in certain ranges of Reynolds numbers. For example, effect of corrugation angle on the heat transfer coefficient for a 20 % solution of glycerin was shown in [2]. When the corrugation angle is changed from 30° to 40°, a 20 % increase in the Nusselt number is obtained compared to a plain tube but further increase in corrugation angle from 40° to 50° results in a fall of this effect to 9 %. Work [3] presents results of experimental studies of a variety of corrugated pipes with various corrugation wavelengths and amplitudes. Increase in hydraulic losses was from 20 % to 300 % compared to a smooth pipe while the Nusselt number increased by 250 %.

In the experimental study [4], all spirally corrugated pipes differing only in corrugation geometry showed a 1.8–2.7 times higher heat transfer in the Reynolds number

range 10^4–$6{\cdot}10^4$ compared to a smooth pipe at a corresponding 2 to 4-fold increase in hydraulic losses.

Numerical modeling of influence of shape of corrugated pipes on their thermal and hydraulic characteristics was carried out for smooth pipes, pipes with undulated goffers and pipes with spiral goffers [5]. For Re=100...1300, the spirally corrugated pipe showed the best thermal characteristics among other types of corrugated pipes: heat exchange growth in it was 18.4–36.3 % compared to a smooth pipe. Straight round goffers were found the least effective.

A special feature of studies of spiral corrugation carried out by the authors of works [5, 6] is consideration of water property variability as a function of temperature. According to the results of numerical simulation with a Reynolds number of 100–700 presented in work [6], heat transfer increased by 21.7–60.5 % with an increase in the coefficient of hydraulic losses by 19.2–36.4 %.

Beside round and undulated corrugation, there are also V-shaped corrugation [7], M-like corrugation [8], etc. In these works, availability of heat exchange intensification in a certain range of Reynolds numbers was shown. At the same time, no correlation was found between the flow structure and intensification of heat transfer for the dropping liquid when thermophysical properties of the heat carrier and geometry of the pipe surface change. Therefore, emphasis was placed on the interrelation between heat transfer on the surface of a complex shape and the structure of a vortex flow taking into account variation of physical properties of the heat carrier.

3. The study objective and tasks

This study objective was to determine conditions for intensification of heat exchange of internal flows while minimizing hydraulic losses.

To achieve this goal, the following tasks were set:

– investigate changes in local heat transfer and flow structure resulted from geometric parameters of the surface in the considered range of Reynolds numbers;

– determine dependence of thermohydraulic parameters of the internal flow on the heat flow direction in the inlet pipe section and dependence of physical characteristics of the heat carrier on temperature;

– study the flow stability depending on geometry of the corrugated pipe surface in the inlet pipe section in the Reynolds number range under consideration.

4. Setting of the numerical experiment in a pipe with a corrugated insert

Axisymmetric flow of a viscous heat-conducting incompressible medium (water) in a pipe with a corrugated insert of finite length was considered.

Fig. 1 shows geometry of the studied pipe of radius R_0=35 mm which consists of an inlet pipe branch, a corrugated insert and an outlet pipe branch.

Symmetric sinusoidal corrugation was considered relative to the radius R_0+a where a=3 mm is the sinusoid amplitude. Such corrugation has no local radii less than R_0.

The geometric characteristics of the corrugated insert are given in Table 1.

Table 1

Geometric parameters of corrugated inserts

L, mm	L/R_0	Corrugated insert surface area, m^2	Outlet pipe branch surface area, m^2
10	0.29	0.108	0.299
20	0.57	0.080	0.299
30	0.86	0.070	0.301
40	1.14	0.070	0.299
60	1.71	0.073	0.295

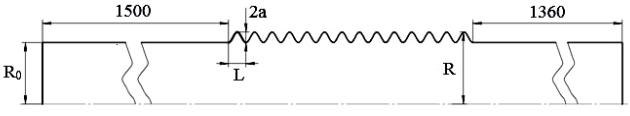

Fig. 1. Geometry of the studied pipe

Study of the viscous heat-conducting fluid was carried out on the basis of a classical system of equations written in an axisymmetric form [9]:

$$\rho\left(\frac{\partial V_r}{\partial \tau}+V_r\frac{\partial V_r}{\partial r}+V_z\frac{\partial V_z}{\partial z}\right)=$$
$$=-\frac{\partial P}{\partial r}+\left(\frac{\partial}{\partial r}\left(\mu\frac{\partial V_r}{\partial r}\right)+\frac{\mu}{r}\frac{\partial V_r}{\partial r}-\frac{\mu V_r}{r^2}+\frac{\partial}{\partial z}\left(\mu\frac{\partial V_r}{\partial z}\right)\right), \quad (1)$$

$$\rho\left(\frac{\partial V_z}{\partial \tau}+V_r\frac{\partial V_z}{\partial r}+V_z\frac{\partial V_z}{\partial z}\right)=$$
$$=-\frac{\partial P}{\partial z}+\left(\frac{\partial}{\partial r}\left(\mu\frac{\partial V_z}{\partial r}\right)+\frac{\mu}{r}\frac{\partial V_z}{\partial r}+\frac{\partial}{\partial z}\left(\mu\frac{\partial V_z}{\partial z}\right)\right), \quad (2)$$

$$\frac{1}{r}\frac{\partial(rV_r)}{\partial r}+\frac{\partial V_z}{\partial z}=0, \quad (3)$$

$$\rho Cp\left(\frac{\partial T}{\partial \tau}+V_r\frac{\partial T}{\partial r}+V_z\frac{\partial T}{\partial z}\right)=\lambda\left(\frac{\partial^2 T}{\partial r^2}+\frac{1}{r}\frac{\partial T}{\partial r}+\frac{\partial^2 T}{\partial z^2}\right), \quad (4)$$

where μ is the coefficient of dynamic viscosity represented by a polynomial of the 2nd degree:

$$\mu = 2{,}791\cdot10^{-7}\cdot T^2-1{,}8\cdot10^{-4}\cdot T+0{,}03231448 \text{ [10].}$$

The following boundary conditions were used when carrying out numerical experiment:

– average-flow velocity and temperature of the heat carrier are set at the inlet;

– "outflow" condition is set at the outlet section;

– condition of adhesion and constant temperature are set for the pipe surface.

The range of average-flow velocities of the heat carrier was V=0.03...0.1 m/s which corresponds to the range of Reynolds numbers $2.3{\cdot}10^3$–$1.4{\cdot}10^4$ and Prandtl numbers Pr=9.41 ... 3,00 in the considered temperature range of the heat carrier from 10 °C to 60 °C.

Simulation was carried out at several combinations of temperatures of the heat carrier and the wall. The value of the set inlet temperature was varied: 60, 35, 10 °C. For spec-

ified boundary conditions of the first kind, a temperature head of ±50 °C and ±25 °C was provided.

There was impact inlet to the pipe, that is the velocity value was the same across the entire inlet section of the pipe, which significantly overrates the values of stresses and heat fluxes in the inlet section of the pipe surface in comparison with their values for asymptotic steady flow, which is usually realized at a distance of 40–50 diameters from the inlet section of the pipe.

The problem was solved numerically with the help of Fluent software package in combination with the Gambit generator of computational grids. A fragment of the structured grid is shown in Fig. 2.

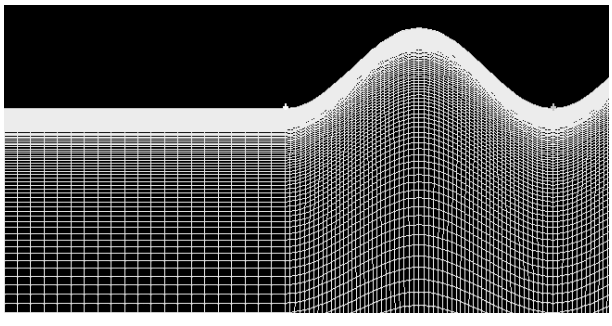

Рис. 2. Fragment of the structured grid of the calculation region

A structured grid thickening in the direction of the pipe wall was constructed. In the zone of the corrugated insert, the computational grid had smaller cells for a more detailed study of the flow structure.

5. Results of studies of the thermal-hydraulic characteristics of pipes with corrugated inserts under the transient flow conditions

5. 1. Influence of temperature head and Reynolds number

Fig. 3 shows distribution of values of dimensionless pressure along the axis of the pipe with a corrugated insert (wavelength L=20 mm) for various values of the modulus and direction of the heat flow vector.

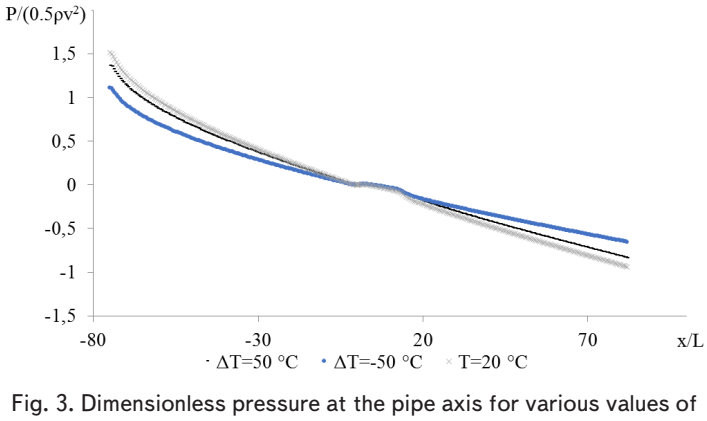

Fig. 3. Dimensionless pressure at the pipe axis for various values of temperature head and Reynolds number of $4.43 \cdot 10^3$

The smallest pressure change was observed with hot walls and cold heat carrier (ΔT=–50 °C). With cold walls and hot heat carrier (ΔT=+50 °C), hydraulic resistance in the pipe was higher but its value was lower than for isothermal flow (T=20 °C) which indicates effect of the dynamic viscosity gradient along the normal to the surface.

In the corrugated pipe section, there was a slight local increase in pressure at the pipe axis due to the pipe surface geometry. In this case, pressure on the goffer wall oscillated around the values of the pressure at the axis (Fig. 4) which determines additional resistance when the pressure values are asymmetric on the symmetrical goffer surface.

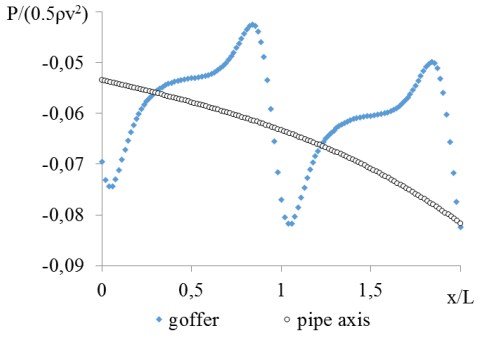

Fig. 4. Dimensionless pressure on the walls and at the pipe axis at two wavelengths of the corrugated section with Reynolds number of $4.43 \cdot 10^3$, ΔT=+50 °C

Minimum and maximum pressure values were observed in the region of the goffer apexes: minimum was behind the apex and maximum was ahead the apex where the current line branches into an internal current in the cavity and a sliding external current. Fig. 5 shows the vector flow field in the cavity where the arrows indicate regions of the largest shear stress values. Amplitudes of pressure oscillations on the pipe surface relative to the value at the axis were practically equal in each subsequent corrugation, which indicates flow regularity inside the goffer.

A stable circulation flow was observed in the corrugation cavity. Negative values of shear stress corresponded to this flow. A sharp change in the values of shear stress on the surface of the corrugated pipe section was due to a vortex flow inside the cavity. The stress values on the surface were analogous to the pressure gradient distribution, the largest values of shear stresses were observed at the goffer vertices. On the windward wall of each cavity in the corrugated insert, there was a point at which flow "stops" and there is practically no boundary layer near this point. The flow behaved here like in an "impact" entry into the pipe when the flow was not yet developed and the boundary layer was minimal. Fig. 6 shows distribution of shear stresses on the surface of the first two and the last two cavities of the corrugated insert.

In the range of Reynolds numbers under consideration, a stable circulation flow in the goffer cavities determined negative shear stress on their surface inside the goffer.

The change in the sign of the temperature flux has a great influence on the velocity profile formation in the pipe. The velocity profile was the most filled with a hot wall and a cold heat carrier, while the maximum velocity gradient shifted away from the wall with a cold wall and a hot heat carrier (Fig. 7).

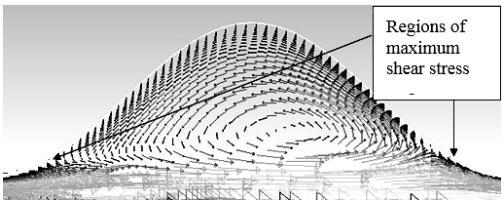

Fig. 5. Flow in the corrugated insert cavity at Reynolds number $4.43 \cdot 10^3$, $\Delta T=+50$ °C

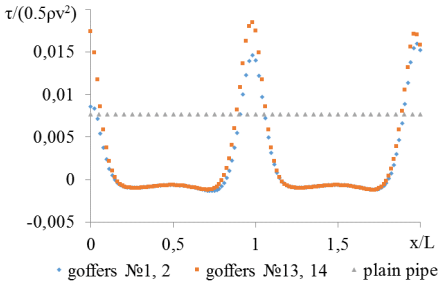

Fig. 6. Dimensionless shear stress on the surface of the corrugated section of the pipe surface at a Reynolds number of $4.43 \cdot 10^3$, $\Delta T=+50$ °C

The obtained character of velocity distribution in the pipe was caused by the heat carrier temperature gradient along the normal to the pipe wall and, consequently, by the changing dynamic viscosity. For water, smaller local viscosity values correspond to higher temperatures. The realized velocity profile (Fig. 7) can lead to an unstable flow [11] with growth of the temperature gradient and hence the gradient of the dynamic viscosity coefficient for cold surface of the pipe.

Inside the goffer cavities, vorticity distribution was practically independent of the value of the temperature head modulus since it was determined only by the wall temperature.

Steady circulation movement in the goffer cavities at low speeds when there is practically no liquid exchange between the flow core and the circulation flow inside the cavities creates a uniform temperature zone determined by the wall temperature. In this connection, values of the heat transfer coefficient are significantly reduced (up to 6 times) as compared to the heat transfer coefficient at the non-corrugated section of the pipe. In the area of junction of the cavities in the regions of maximum stresses, the boundary thermal layer was most thin, hence, thermal resistance was smallest in these zones which explains the increase (two-fold in comparison with the plain pipe) in the heat transfer values (Fig. 8).

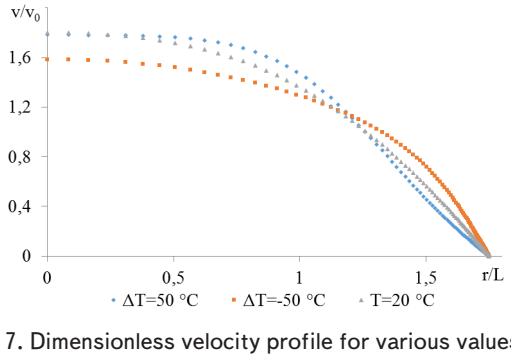

Fig. 7. Dimensionless velocity profile for various values of the temperature gradient at a Reynolds number of $4.43 \cdot 10^3$

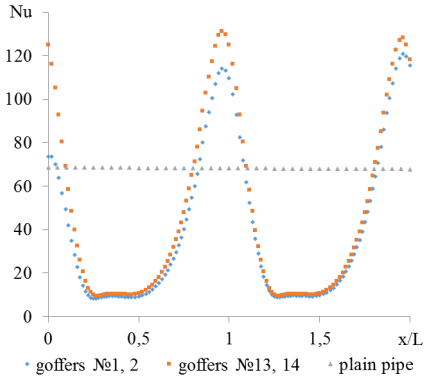

Fig. 8. Dependence of the Nusselt number on a dimensionless coordinate in a corrugated insert at Reynolds number of $4.43 \cdot 10^3$, $\Delta T=+50$ °C

Direction of the heat flux vector relative to the surface of the pipe influences intensity of heat transfer as well. With cold heat carrier and hot wall surface ($\Delta T=-50$ °C), heat flow in each section of the pipe in the Reynolds number range under consideration was higher than in the case of hot heat carrier and cold surface ($\Delta T=+50$ °C) with a corresponding Reynolds number (Table 2). Besides, the heat flux increment (25–30 %) in the corrugated section was somewhat larger than in the outlet branch pipe (17–18 %) and this difference increased with increase of the Reynolds number (Table 2).

Table 2

Heat flows in a pipe with a corrugated insert $L/R_0=0.57$

Reynolds number	Heat flows, W			Section of the outlet branch pipe undergoing influence of the corrugated insert, S related to the corrugation wave length, S/L	Temperature head, °C
	Corrugation	Outlet branch pipe	Entire pipe		
Re=4430	162.79	826.68	3015.14	45.05	ΔT=50
	201.49	966.13	3611.27	15.65	ΔT=–50
Re=14770	290.92	1408.41	5214.73	60.00	ΔT=50
	388.20	1662.44	6349.45	17.25	ΔT=–50

With the growth of the Re numbers, the zone of stable circulation flow is destroyed and it is necessary to proceed to solution of the problem in a non-stationary statement.

5. 2. Effect of the corrugated insert wavelength

When analyzing influence of the cavity parameters on the vortex structure, the length and depth of the cavities are always correlated with the thickness of the boundary layer. These two parameters determine vortex structure of the flow inside the cavities and in the trace behind them [12].

For internal flows in the pipe, two additional parameters must also be taken into account in modeling: corrugation wavelength and amplitude correlated with the pipe radius (Table 1).

Analysis of the effect of the corrugation wavelength on the flow structure based of the stationary solution showed that structure of the vortex flow inside the cave changes with increase in the corrugation wavelength. Thus, upon reaching

$$\mathrm{Re}_L = \frac{v \cdot L}{\nu} \approx 2500,$$

integral circulation flow in the cavity transforms into a multi-vortex structure with an irregular mass exchange between the cavity and the main flow in the pipe which indicates that the stationary solution is limited for Reynolds numbers exceeding the threshold value. Fig. 9 shows the values of the radial velocity component at the interface "main flow – cavity". Mass exchange between the fluid in the goffer cavities and the main flow of the heat carrier appears at $L/R_0>0.6$ and increases with a further increase in the corrugation wavelength which is confirmed by the values of the radial velocity component at the interface.

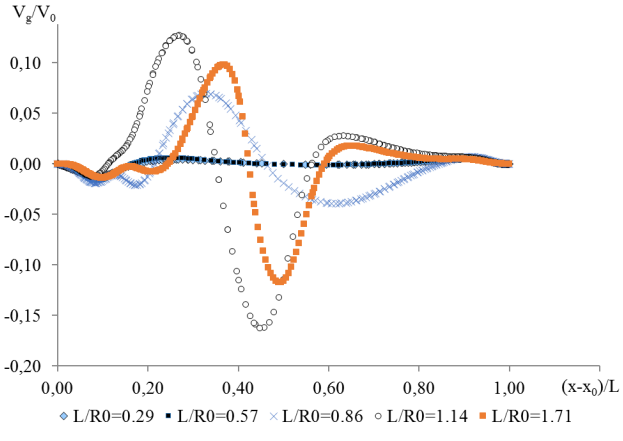

Fig. 9. Radial component of velocity at the interface "main flow-cavity" at a Reynolds number of $1.4\cdot10^4$, $\Delta T=+50$ °C with a change in the cavity length

As the corrugation wavelength increases, amplitudes of the radial velocity component grow. In this case, maximum positive velocity values are shifted to the beginning of the cavity and the maximum negative velocity components are located near the middle of cavities, which indicates localization of the main vortex at the beginning of the cavity.

A change in the vortex flow structure with an increase in the corrugation wavelength at $Re=1.4\cdot10^4$ leads to an intensification of heat and mass exchange inside the cavity (Table 3).

Table 3

Heat flows in the pipe at $Re=1.4\cdot10^4$, $\Delta T=+50$ °C

Density of heat flows in various locations of the pipe surface, W/m^2	$L/R_0=0.29$	$L/R_0=0.57$	$L/R_0=0.86$	$L/R_0=1.14$	$L/R_0=1.71$
Corrugated insert	3718.53	3788.58	5282.32	4810.45	5207.22
Inlet pipe branch	8504.80	8504.78	8506.22	8506.75	8505.63
Outlet pipe branch	4714.48	4709.84	4951.69	5027.33	4965.99

The values of the heat flows passing the pipe surface essentially depend on the flow structure due to the cavity parameters. Thus, starting with $L/R_0=0.86$, the flow vortex structure in the goffer cavity (Fig. 9) causes oscillations in the heat fluxes in the corrugated section. In the outlet pipe branch downstream the corrugated section, intensification of heat transfer takes place ranging from 4 % to 11 % which is caused by generation of vortex formations in the goffer cavities and their subsequent downstream transport.

If the Reynolds number exceeds 7,000–10,000, it is impossible to obtain steady-state values of flow characteristics in the pipe for any corrugation wavelengths at the stationary problem statement. Amplitude of oscillation of the characteristics of velocity, pressure, and temperature remain finite, which indicates occurrence and destruction of vortex structures inside cavities and their transportation in the outlet branch pipe.

Non-stationary problem formulation makes it possible to trace arising oscillations and analyze their variation in time. If there is a discrete spectrum of changing flow characteristics, one can speak of a quasi-periodicity of the flow with sufficiently large pressure difference oscillations: up to 20 % of the averaged pressure difference. The change in the pressure difference is determined by generation of vorticity perturbations in the cavities, which determines pressure perturbation downstream.

Analysis of the spectra of pressure oscillations downstream the corrugated pipe section showed that the number of discrete spectrum components increases with increase in corrugation wavelength. Thus, only one discrete frequency of ~1 Hz is observed at L=10 mm and three discrete frequencies (~0.5 Hz, ~1 Hz, ~2 Hz) can be fairly clearly identified at L=40 mm.

Similar frequency dependence was observed in an unsteady heat flow at the outlet of the pipe due to the movement of vortices downstream. With an increase in the corrugation wavelength, intensity of heat transfer increases but when the corrugation wavelength reaches $L/R_0=0.85$, heat transfer ceases to change (Fig. 10).

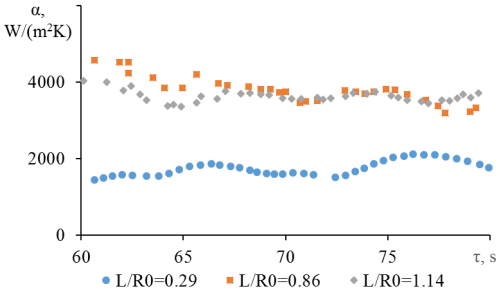

Fig. 10. Heat transfer coefficient depending on the length of the goffer cavity at a Reynolds number $1.4\cdot10^4$, $\Delta T=+50$ °C

Numerical experiment showed intensification of heat emission in a pipe with a corrugated insert of an order of 1.1–1.3 times, which correlates with the experimental data [3] (Fig. 11).

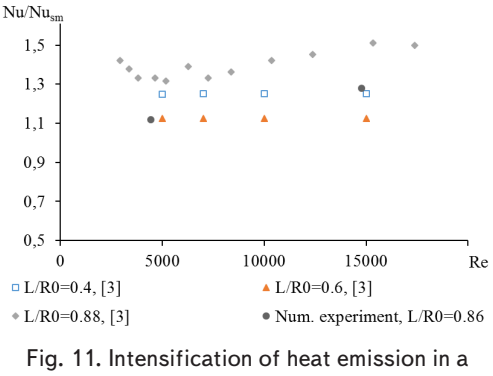

Fig. 11. Intensification of heat emission in a pipe with a corrugated insert in comparison with a plain pipe (non-stationary regime) depending on the Reynolds number, $\Delta T=+50$ °C

It should be noted that results were presented in [3] for a pipe with corrugation along its entire length in which intensification of heat transfer was obtained at a significantly increased resistance (by a factor of 1.5), while for the pipes studied with a non-clogging corrugated insert, the ratio of

the hydraulic resistance of the pipe with the insert to the resistance of the plain pipe did not exceed 5 % at ΔT=+50 °C.

6. Discussion of the results obtained in the study of pipes with corrugated inserts

The results of numerical simulation have shown that the local heat emission essentially depends not only on the Reynolds and Prandtl numbers, but also on the goffer geometry and direction of the heat flux.

Length of the dynamic inlet section at a flow of dropping liquid (Pr>1) in the pipe and boundary condition $T_w \neq T_f$ was much larger than the length of the inlet section at $T_w=T_f$. Length of the inlet section of thermal boundary layer substantially exceeds length of dynamic boundary layer. Presence of a corrugated insert increases length of the inlet section.

On the hot surface of the pipe ($T_w>T_f$), the heat exchange was more intensive in comparison with the cold surface ($T_w<T_f$) at the same value of the temperature head modulus magnitude $\Delta T = |T_f - T_w|$ and proportional to its value throughout the range of Reynolds numbers considered.

At Reynolds numbers greater than 7,000–10,000, steady flow in the pipe was not realized for a non-isothermal formulation of the problem while the flow remained laminar at $T_w=T_f$.

The local heat transfer coefficient changed sharply along the length of wave of the surface goffer, e. g. the ratio of the coefficient at the goffer cavities to the coefficient at the goffer peaks was 1/12.

With an increase in the corrugation wavelength, a qualitative change in the flow structure in the cavity occurs at a fixed Reynolds number: low-frequency ejections from the cavities arise which significantly intensifies heat exchange (up to 1.3 times).

Numerical simulation makes it possible to evaluate influence of one or another factor of heat exchange intensification, reveal the range of parameters of the most effective method of heat exchange intensification and estimate the energy costs for ensuring the corresponding intensification. The considered range of pipe parameters and flow rates is most suitable for heat pumps. These studies can be continued with an extension of the range of Reynolds numbers and taking into account flow chaotization.

7. Conclusions

1. The use of corrugated surfaces is not effective at Reynolds numbers Re<2000.

2. The use of nonencumbering corrugation makes it possible to rise heat exchange up to 30 % with an increase in hydraulic resistance by 1.05 times in the range of Reynolds numbers $2 \cdot 10^3 ... 1.4 \cdot 10^4$.

3. Interrelation between the heat transfer intensification in the corrugated section and variation of the wave length of corrugation was shown. Threshold value of the corrugation wavelength ($L/R_0>0.6$) was found in the considered range of Reynolds numbers for which a significant increase in heat exchange occurs.

4. Classical results of the effect of the heat flux direction on the value of heat exchange coefficients were numerically confirmed. Peculiarities of the vortex flow structure were revealed which manifest themselves when considering variability of the coefficient of viscosity depending on the temperature in a more intensive vortex formation, which affects intensity of the heat exchange processes in the pipe downstream the corrugated insert.

References

1. Nyarko, P. Heat Load and its Effects on Fluid Friction Factor in Corrugated Pipes [Text] / P. Nyarko // American Journal of Scientific and Industrial Research. – 2012. – Vol. 3, Issue 4. – P. 241–251. doi: 10.5251/ajsir.2012.3.4.241.251
2. Sreedhara Rao, B. Effect of corrugation angle on heat transfer studies of viscous fluids in corrugated plate heat exchangers [Text] / B. Sreedhara Rao, D. Surywanshi Gajanan, S. Varun, M. V. S. Murali Krishna, R. C. Sastry // International Journal of Engineering and Technology Innovation. – 2015. – Vol. 5, Issue 2. – P. 99–107.
3. Vicente, P. G. Experimental investigation on heat transfer and frictional characteristics of spirally corrugated tubes in turbulent flow at different Prandtl numbers [Text] / P. G. Vicente, A. Garcia, A. Viedma // International Journal of Heat and Mass Transfer. – 2004. – Vol. 47, Issue 4. – P. 671–681. doi: 10.1016/j.ijheatmasstransfer.2003.08.005
4. Zimparov, V. D. Heat transfer and friction characteristics of spirally corrugated tubes for power plant condensers – 1. Experimental investigation and performance evaluation [Text] / V. D. Zimparov, N. L. Vulchanov, L. B. Delov // International Journal of Heat and Mass Transfer. – 1990. – Vol. 34, Issue 9. – P. 2187–2197. doi: 10.1016/0017-9310(91)90045-g
5. Nazri, M. N. Corrugation profile effect on heat transfer enhancement of laminar flow region [Text] / M. N. Nazri, T. M. Lazim, S. Abdulla, Z. S. Kaeem, A. F. Abdulwahd // International Conference on Mechanical And Industrial Engineering (ICMAIE'2015). – Kuala Lumpur (Malaysia), 2015. – P. 93–98. doi: 10.15242/iae.iae0215218
6. Kareem, Z. S. Heat transfer enhancement in two-start spirally corrugated tube [Text] / Z. S. Kareem, M. N. Mohd Jaafar, T. M. Lazim, S. Abdullah, A. F. AbdulWahid // Alexandria Engineering Journal. – 2015. – Vol. 54, Issue 3. – P. 415–422. doi: 10.1016/j.aej.2015.04.001
7. Noor, S. Heat transfer and pumping power using nanofluid in a corrugated tube [Text] / S. Noor, M. M. Ehsan, S. Salehin, A. K. M. Sadrul Islam // 19th Australasian Fluid Mechanics Conference. – Melbourne, Australia, 2014.
8. Sibley, K. J. Heat transfer coefficient for air flow in plastic drainage tubes [Text] / K. J. Sibley, G. S. V. Raghavan // Canadian agricultural engineering. – 1984. – Vol. 26, Issue 2. – P. 177–180.
9. Loycyanskiy, L. G. Mekhanika zhidkosti i gaza [Text] / L. G. Loycyanskiy. – Moscow: Gosudarstvennoe izdatel'stvo tekhniko-teoreticheskoy literatury, 1950. – 680 p.
10. Rivkin, S. L. Termodinamicheskie svoystva vody i vodyanogo para [Text] / S. L. Rivkin, A. A. Aleksandrov. – 2-e izd., pererab. i dop. – Moscow: Energoatomizdat, 1984. – 80 p.
11. Lin', C.-C. Teoriya gidrodinamicheskoy ustoychivosti [Text] / C.-C. Lin'. – Moscow: Izdatel'stvo inostrannoy literatury, 1958. – 195 p.
12. Voropaev, G. A. Chislennoe modelirovanie vyazkogo techeniya nad poverhnost'yu s uglubleniem [Text] / G. A. Voropaev, N. V. Rozumnyuk // Prikladna gidromekhanika. – 2004. – Vol. 6, Issue 4. – P. 17–23.